

# A residue in the middle of the M2-M3 loop of the $\beta_4$ subunit specifically affects gating of neuronal nicotinic receptors

José Carlos Rovira<sup>a</sup>, Juan José Ballesta<sup>a</sup>, Francisco Vicente-Agulló<sup>b</sup>, Antonio Campos-Caro<sup>b</sup>, Manuel Criado<sup>b</sup>, Francisco Sala<sup>b,\*</sup>, Salvador Sala<sup>c</sup>

<sup>a</sup>Departamento de Farmacología, Instituto de Neurociencias, Universidad Miguel Hernández, Campus de San Juan, Aptdo. Correos 18, 03550 San Juan, Alicante, Spain

<sup>b</sup>Departamento de Neuroquímica, Instituto de Neurociencias, Universidad Miguel Hernández, Campus de San Juan, Aptdo. Correos 18, 03550 San Juan, Alicante, Spain

<sup>c</sup>Departamento de Fisiología, Instituto de Neurociencias, Universidad Miguel Hernández, Campus de San Juan, Aptdo. Correos 18, 03550 San Juan, Alicante, Spain

Received 15 June 1998

**Abstract** An aspartate residue in the M2-M3 loop of neuronal nicotinic receptor  $\alpha_7$  subunits is a major determinant of the channel functional response. This residue is conserved in most  $\beta_4$  subunits, e.g. human and rat, but not in others, e.g. bovine. We have used these differences to examine the mechanism by which this residue alters the functional properties of  $\alpha_3\beta_4$  receptors. Having ruled out an effect on the macroscopic binding ability of the agonist, the level of receptor expression, or the single channel conductance, the results suggest that receptors lacking that residue have a deficient coupling between binding and gating.

© 1998 Federation of European Biochemical Societies.

**Key words:** Neuronal nicotinic receptor;  $\alpha_3\beta_4$  Receptor; Binding and gating coupling; Single-channel conductance

## 1. Introduction

In a previous work [1] we found that an Asp residue located in the middle of the M2-M3 loop reduced maximal currents in both homomeric  $\alpha_7$  and heteromeric  $\alpha_3\beta_4$  receptors. In the latter case, however, we could not establish the level of expression of the receptors and the possibility remained open that, contrasting with  $\alpha_7$ , the effect of the mutation was primarily on the ability of the cell to express membrane receptors and not on their function. Even with  $\alpha_7$  receptors, the possibility of an effect of the mutations on the elementary conductance could not be ruled out at that time, since single channel recordings in oocytes expressing  $\alpha_7$  are difficult to obtain, probably because of clustering [2].

Although human and rat  $\beta_2$  and  $\beta_4$  subunits have an Asp residue in the M2-M3 loop, this is not a conserved feature of each  $\beta$ -type subunit. For example, bovine  $\beta_4$  subunits have an Asn residue in the equivalent position [3]. Thus, using mutants of bovine and rat  $\beta_4$  subunits we have studied both the effect of removing the Asp, by mutating the rat subunit (D268A mutation), or adding it, by mutating the bovine subunit (N268D mutation). In addition, the use of  $\alpha_3\beta_4$  receptors had the advantage over  $\alpha_7$  receptors of allowing single channel recordings in oocytes.

In this work we present data of expression and single chan-

nel recordings of  $\alpha_3\beta_4$  receptors expressed in *Xenopus* oocytes and composed of bovine  $\alpha_3$  and rat or bovine  $\beta_4$  subunits providing evidence that the residue located at position 268 in the loop M2-M3 of the  $\beta_4$  subunit ( $\beta_4$ 268) affects gating in neuronal nicotinic receptors.

## 2. Materials and methods

### 2.1. Site-directed mutagenesis and oocyte expression

Point mutations were made by performing two successive PCR amplifications as described [4,5] and were confirmed by sequencing the cDNA clones. DNAs were inserted into the pSP64T vector [6]. Capped mRNA was synthesized in vitro using SP6 RNA polymerase. Defolliculated *Xenopus* oocytes were injected with 5 ng of total RNA in 50 nl of sterile water. The two subunits,  $\alpha_3$  and  $\beta_4$ , were injected in an equimolar ratio. All measurements were made within 3–6 days after injection.

### 2.2. Epibatidine binding assays

Oocyte microsomal fraction was obtained as described [7] with minor modifications. [<sup>3</sup>H]Epibatidine binding saturation experiments were performed with the microsomal fraction as described [8]. To obtain  $B_{\max}$  and  $K_d$  parameters, data were analyzed with LIGAND, a non-linear least squares computer program for ligand binding systems [9].

To determine oocyte surface [<sup>3</sup>H]epibatidine binding, oocytes were preincubated for 2 h at 4°C with either Barth buffer (total binding), or 0.5 mM D-tubocurarine in the above buffer (internal binding, since this antagonist cannot permeate the oocyte membrane, as happens with epibatidine) or 100 nM unlabelled epibatidine (non-specific binding). At the end of the preincubation period, [<sup>3</sup>H]epibatidine was added (2 nM final concentration) and the oocytes were incubated as above during 4 h. After that period, unbound epibatidine was eliminated by aspiration and oocytes were washed 4 times in ice-cold Barth buffer. Then, oocytes were homogenized, solubilized and immunoprecipitated with mAb35 as described [10]. Radioactivity remaining in the immunoprecipitate was measured in a liquid scintillation counter. Oocyte surface [<sup>3</sup>H]epibatidine binding was calculated by subtracting the specific cpm obtained for the total and internal binding. The number of surface [<sup>3</sup>H]epibatidine binding sites (in pmol/mg protein of microsomal fraction) was calculated by multiplying  $B_{\max}$  by the ratio of (surface/total) specific binding.

### 2.3. Electrophysiological recordings

**2.3.1. Macroscopic currents.** Two electrode voltage clamp recordings were obtained as described [1]. Oocytes were perfused with normal frog Ringer solution (NFR) containing (in mM): 115 NaCl, 2.5 KCl, 1.8 CaCl<sub>2</sub>, and 10 HEPES (pH 7.2). Holding potential was –40 mV. At this potential we found no significant difference when BAPTA was injected into the oocytes to avoid calcium-activated chloride currents, and data obtained with or without BAPTA were pooled together. Currents were filtered at 50 Hz with a low pass 8 pole Bessel filter (Frequency Devices, Haverhill, MA), sampled at 500 Hz and stored on hard disk. Data acquisition and agonist application were con-

\*Corresponding author. Fax: (34) (6) 591-9492.  
E-mail: fsala@umh.es

trolled by a DigiData 1200 interface driven by PClamp 6.0.3 software (Axon Instruments, Foster City, CA).

**2.3.2. Single channel currents.** Records were obtained in the cell-attached mode using an Axopatch 200A amplifier (Axon Instruments). Previous to patch-clamp recording, oocytes were screened by two electrode voltage clamp for the presence of nicotine activated currents. Oocytes were bathed in a modified NFR where NaCl was substituted by KCl to clamp the membrane potential close to 0 mV. Holding potential was  $-80$  mV. Patch pipettes were pulled from thick-walled borosilicate glass (GC150-15, Clark Electromedical Instruments), with a resistance of  $5\text{--}10\text{ M}\Omega$  when filled with NFR. Nicotine  $1\text{ }\mu\text{M}$  was added to the pipette solution. Initially  $10\text{ }\mu\text{M}$  gadolinium was added to the pipette to block stretch activated channels [11], but in later experiments gadolinium was not used because nicotine activated receptors could be recognized by their kinetics and conductance range. No such channels were observed neither in control oocytes, nor in injected oocytes when nicotine was not present in the pipette. Records were low-pass filtered at  $1\text{ kHz}$ , sampled at  $5\text{ kHz}$  and stored on hard disk for later analysis.

Single channel recordings were analyzed with the FETCHAN routine of PClamp 6.0 software. Events less than or equal to  $0.2\text{ ms}$  were ignored. The critical shut time for the definition of bursts was calculated as described [12]. Corrections for missed events (dead time =  $0.2\text{ ms}$ ) were applied as in [12].

Data are presented as mean  $\pm$  standard error. Statistical significance was calculated by Student's *t*-test with  $P < 0.05$ .

### 3. Results

#### 3.1. Macroscopic currents and receptor expression

Fig. 1A shows currents elicited by application of  $300\text{ }\mu\text{M}$  nicotine on oocytes expressing receptors composed of bovine  $\alpha_3$  subunit together with either rat or bovine  $\beta_4$  subunits, and the corresponding mutations at position  $\beta_4 268$ . Records are representative of the mean value observed for each receptor. Fig. 1C shows the mean current obtained averaging the results from eight different donors. For each donor, 20 oocytes were measured.

The mutation D268A produced a reduction of the current of approximately 3-fold, and the mutation N268D produced the reverse effect. Similar changes in the maximal currents were found for two additional nicotinic agonists (acetylcholine (ACh) and dimethylphenylpiperazinium (DMPP), data not shown).

In order to check for a possible effect of mutations on apparent affinity of the receptor for nicotine, macroscopic dose-response curves in the range between  $1\text{ }\mu\text{M}$  and  $1\text{ mM}$  were measured in 4–7 oocytes from 2–3 donors (Fig. 1B). The data point corresponding to  $1\text{ mM}$  usually gave lower than maximal currents, probably due to self-inhibition [13], and only data in the range of  $1\text{--}300\text{ }\mu\text{M}$  were fitted to the Hill equation. The  $\text{EC}_{50}$  and Hill coefficient did not show significant differences between wild type and mutated receptors. We previously obtained similar results in rat receptors measured at  $-80\text{ mV}$  with nicotine, ACh and DMPP [1].

Furthermore, mutations in  $\beta_4 268$  did not affect the apparent affinity of desensitized receptors for epibatidine as measured in saturation experiments,  $K_d$  (in nM): rat  $0.80 \pm 0.14$ ; D268A  $1.45 \pm 0.78$ ; bovine  $1.80 \pm 0.57$ ; N268D  $0.54 \pm 0.11$  ( $n = 3$ , statistically non-significant differences).

The change in macroscopic current produced by the mutations could be due to a change in (a) the expression of receptors, (b) the elementary conductance, or (c) the open probability of the receptor, or a combination of these. We studied each of these possibilities.

Differences in expression as determined by [ $^3\text{H}$ ]epibatidine

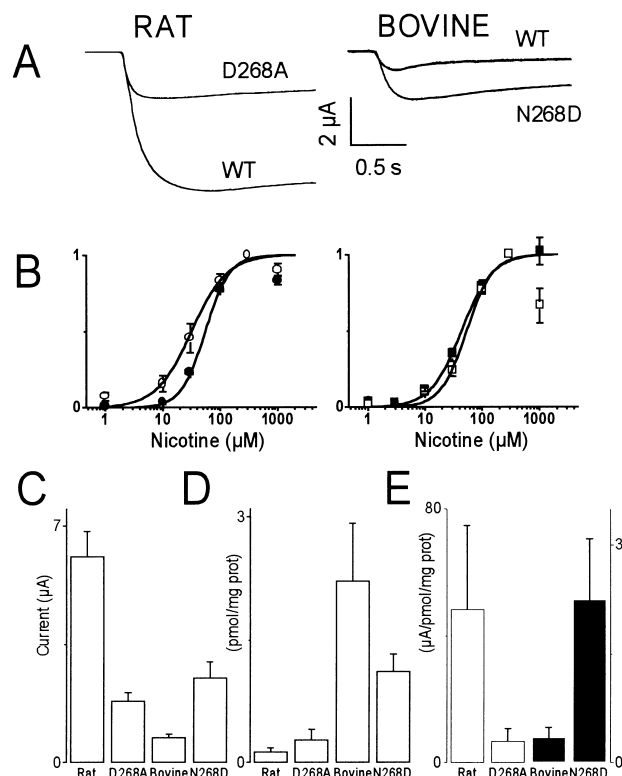


Fig. 1. Macroscopic currents and surface expression of  $\alpha_3\beta_4$  receptors. A: Current records obtained upon application of  $300\text{ }\mu\text{M}$  nicotine. B: Dose-response curves for nicotine. Fit parameters ( $\text{EC}_{50}$  in  $\mu\text{M}$ , Hill coefficient): rat ( $\circ$ ) ( $33 \pm 3$ ,  $1.5 \pm 0.2$ ), D268A ( $\bullet$ ) ( $54 \pm 2$ ,  $2.1 \pm 0.1$ ); bovine ( $\square$ ) ( $53 \pm 4$ ,  $1.9 \pm 0.2$ ), N268D ( $\blacksquare$ ) ( $43 \pm 3$ ,  $1.6 \pm 0.2$ ). C: Mean current for each receptor at  $300\text{ }\mu\text{M}$  nicotine. D: [ $^3\text{H}$ ]Epibatidine surface binding for each receptor. E: Current per receptor surface expression level. Different axes are used for rat (white) or bovine (black) receptors.

binding for each mutant receptor when compared with its wild type counterpart (Fig. 1D) do not account for the change in macroscopic currents, rather they make it larger. When maximal currents normalized to receptor expression are considered (Fig. 1E), the mutation D268A produces a 7.2-fold reduction, whereas the mutation N268D produces a 6.7-fold increase.

#### 3.2. Single channel currents

Fig. 2 shows single channel recordings and their corresponding amplitude histograms. Single channel conductances were measured from I-V curves in the range between 0 and  $-120\text{ mV}$ . For all four types of receptors, the current voltage relationship was linear in this voltage range.

As found in other studies on  $\alpha_3\beta_4$  receptors expressed in *Xenopus* oocytes [14,15], there was considerable interpatch variability in the values of the conductance. At the bottom of Fig. 2 the main conductance of successive patches is plotted for the four receptors. The conductance of each receptor was, in pS: rat:  $18.2 \pm 0.46$  ( $n = 38$ ), D268A:  $17.5 \pm 0.94$  ( $n = 11$ ); bovine:  $19.3 \pm 0.59$  ( $n = 27$ ), N268D:  $20.1 \pm 0.81$  ( $n = 20$ ). Means are not statistically different. Hence, neither a change in single channel conductance nor prevalence of a channel with different conductance, which could explain the change in macroscopic currents, was found in mutant receptors.

### 3.3. Single channel kinetics

The above results suggested that a change in the maximum open channel probability (reached at 300  $\mu$ M nicotine) of mutated receptors was responsible for the observed effects.

Single channel currents at 1  $\mu$ M nicotine are shown in Fig. 2, where differences in kinetics between wild type and mutated receptors could be observed, mainly in the open duration.

Although the open probability is low at 1  $\mu$ M nicotine (see amplitude histograms in Fig. 2), it has the advantage of allowing long recordings without desensitization present at 300  $\mu$ M nicotine. Furthermore, in most kinetic models used to describe the behavior of nicotinic receptors [16] burst kinetics are determined by rate constants independent of agonist concentration.

Burst analysis of pooled data from each receptor is shown in Fig. 3. Dwell time histograms of burst duration and gap lengths within bursts are displayed. These histograms could be fitted to a single exponential which give the estimate of the mean times. In general, bursts duration was longer and gap duration was shorter in  $\beta_4$ D268 containing receptors. A min-

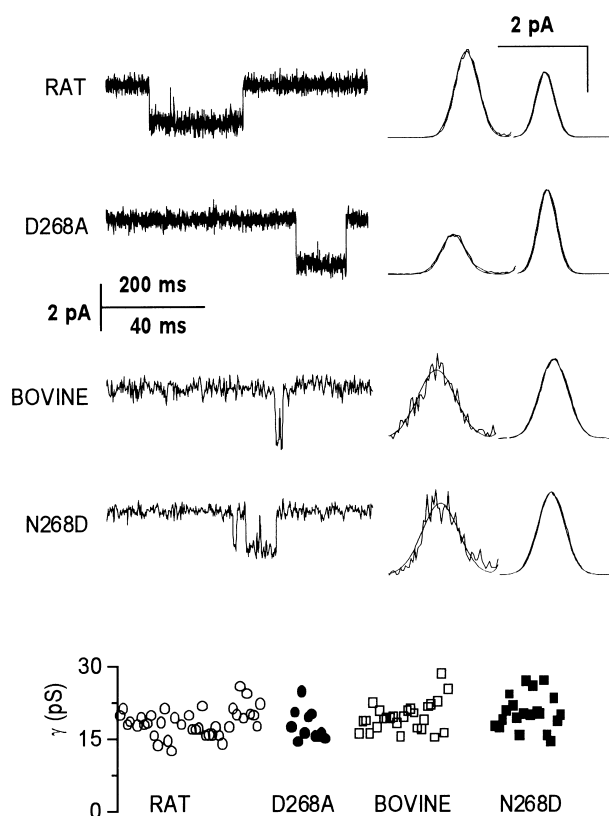


Fig. 2. Conductance of  $\alpha_3\beta_4$  receptors. Left: Sample single channel recordings for each receptor. The records have been chosen so that the lengths of the openings (downward deflections) are close to the average burst duration for each receptor. Note the different time scale for rat and bovine receptors. Right: Amplitude histograms for the same receptors. A period of 60 s was used. Because of the small open probability, two different scales have been used for the baseline and for the openings. The peaks on the right correspond to the baseline and the calibration bar for these is, rat: 15000, bovine: 8750. The peaks on the left correspond to the openings and the calibration bar for these is, rat: 500, bovine: 30. The corresponding gaussian fit is superimposed on each histogram. Bottom: Conductance values of different patches, displayed sequentially as they were measured, for each receptor the number of donors were: rat ( $\circ$ ): 9; D268A ( $\bullet$ ): 4; bovine ( $\square$ ): 5; N268D ( $\blacksquare$ ): 5.

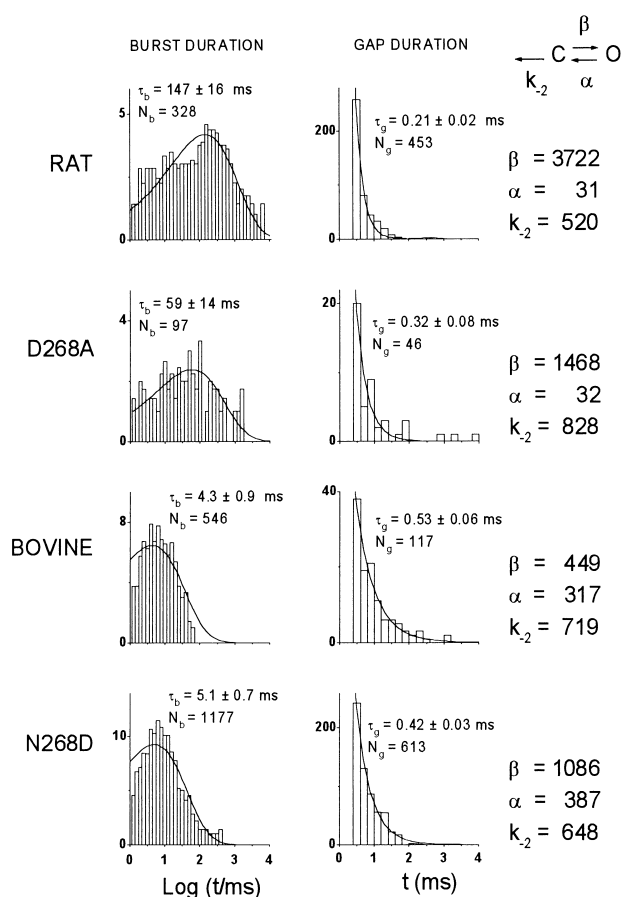


Fig. 3. Dwell time histograms of pooled data of 5–8 patches corresponding to 3–4 donors (5 min recordings per patch). Left: Burst duration histograms for each receptor. A logarithmic binning mode and a square root transformation of the number of events is used in all these histograms. Superimposed is the single exponential fit to the data, and the corresponding time constant.  $N_b$  = total number of bursts in the histogram. Middle: Gaps, or closings within burst, duration histograms for each receptor. In these histograms the conventional binning mode and a linear scale for the number of events was used. Superimposed are the single exponential fit and the corresponding time constant.  $N_g$  = total number of gaps in the histogram. Right: Minimal kinetic model with gating rate constants in  $s^{-1}$ .

imal kinetic scheme including only the last step before opening and the corresponding gating rate constants is also shown. Rate constants have been calculated from the data given in the histograms after correction for missed events [12,16] and are shown (in  $s^{-1}$ ) at the right of each panel.

### 4. Discussion

In this report, we have studied the possible mechanisms by which the presence of an Asp residue at  $\beta_4$ 268 determines larger macroscopic currents in  $\alpha_3\beta_4$  receptors. Differences in surface expression or single channel conductance have been discarded, the latter result was expected for a residue located far away of the putative pore region [17]. Also, although  $\beta$  subunits have been shown to contribute to agonist and antagonist sensitivities [18–22], macroscopic dose-response curves did not change significantly in mutants, suggesting that the residue present at  $\beta_4$ 268 did not affect the binding step.

A possible effect of the mutated residue on agonist open channel block seems unlikely because (1) it would have greatly

affected the  $EC_{50}$ , and (2) agonist open channel block is usually voltage dependent, and the same extent of change in currents has been found at  $-80$  mV (data not shown).

Similarly, an effect of mutations on receptor desensitization also seems unlikely as macroscopic currents of both wild type and mutants decay with similar kinetics upon stimulation with high agonist concentrations. Furthermore, a change in desensitization from the open state would also have shifted the  $EC_{50}$ .

The above results suggest that mutations at  $\beta_4$ 268 should produce changes in the maximum open probability of the channel. We could not get direct proof of that effect, because cell-attached single channel recordings with high concentrations of agonist show desensitization and inside-out patches run-down. As an alternative approach we have obtained an indirect estimation of the gating behavior by analyzing bursts of openings at low concentrations of agonist.

Our results confirm that single channel kinetics are strongly determined by the  $\beta_4$  subunit [14], as burst durations are very different for receptors composed of rat or bovine  $\beta_4$  subunits. More interestingly, the involvement of residue  $\beta_4$ 268 in channel gating is evidenced by the increased burst duration and reduced gap duration in receptors with  $\beta_4$ D268, corresponding to a larger opening rate constant  $\beta$ . These results suggest that the Asp residue at  $\beta_4$ 268 play a role in the transmission of the signal from binding to gating as it affects the gating rate constants in two different neuronal nicotinic receptors, without affecting agonist binding.

According to the model of gating for the nicotinic receptor proposed by Unwin [23], we could speculate that receptors lacking the Asp residue at  $\beta_4$ 268 would have subunits with more difficulty to rotate and open the channel, i.e. decreased opening rate constant. It has been recently suggested that the M2-M3 loop of ligand gated ion channels could indirectly interact with the ligand binding pocket [24]. This possibility is also supported by experimental data, which suggest the involvement of residues located at the M2-M3 loop in signal transduction of glycine receptors [25].

The investigation of the role of the same structure in the  $\alpha$  subunit and its possible interaction with the  $\beta$  subunit would contribute to establish a more precise molecular basis of the coupling mechanism between binding and gating.

**Acknowledgements:** This work has been supported by grants from Dirección General de Enseñanza Superior: PB95-0683 and PB95-0690. F.V.-A. is the recipient of a predoctoral fellowship from the Ministry of Education of Spain. A.C.-C. is a postdoctoral fellow of

C.S.I.C.-Fundación Bancaja. We thank Mrs. Eva Martínez for her technical assistance, and Jon Lindstrom for the generous gift of mAb35.

## References

- [1] Campos-Caro, A., Sala, S., Ballesta, J.J., Vicente-Agulló, F., Criado, M. and Sala, F. (1996) *Proc. Natl. Acad. Sci. USA* 93, 6118–6123.
- [2] Revah, F., Bertrand, D., Galzi, J.L., Devillers-Thiery, A., Mulle, C., Hussy, N., Bertrand, S., Ballivet, M. and Changeux, J.P. (1991) *Nature* 353, 846–849.
- [3] Campos-Caro, A., Smillie, F.I., Domínguez-del-Toro, E., Rovira, J.C., Vicente-Agulló, F., Chapuli, J., Juiz, J.M., Sala, S., Sala, F., Ballesta, J.J. and Criado, M. (1997) *J. Neurochem.* 68, 488–497.
- [4] Herlitze, S. and Koenen, M. (1990) *Gene* 91, 143–147.
- [5] García-Guzmán, M., Sala, F., Sala, S., Campos-Caro, A. and Criado, M. (1994) *Biochemistry* 33, 15198–15203.
- [6] Krieg, P.A. and Melton, D.A. (1984) *Nucleic Acids Res.* 12, 7057–7070.
- [7] Buller, A.L. and White, M.M. (1992) *Methods Enzymol.* 207, 368–375.
- [8] Houghtling, R.A., Davila-Garcia, M.I. and Kellar, K.J. (1995) *Mol. Pharmacol.* 48, 280–287.
- [9] Munson, P.J. and Rodbard, D. (1980) *Anal. Biochem.* 107, 220–239.
- [10] Anand, R., Conroy, W.G., Schoepfer, R., Whiting, P. and Lindstrom, J. (1991) *J. Biol. Chem.* 266, 11192–11198.
- [11] Yang, X.C. and Sachs, F. (1989) *Science* 243, 1068–1071.
- [12] Colquhoun, D. and Sakmann, B. (1985) *J. Physiol.* 369, 501–557.
- [13] Sine, S.M. and Steinbach, J.H. (1984) *Biophys. J.* 46, 277–283.
- [14] Papke, R.L. and Heinemann, S.F. (1991) *J. Physiol.* 440, 95–112.
- [15] Sivilotti, L.G., McNeil, D.K., Lewis, T.M., Nassar, M.A., Schoepfer, R. and Colquhoun, D. (1997) *J. Physiol.* 500, 123–138.
- [16] Colquhoun, D. and Hawkes, A.G. (1995) in: *Single-Channel Recording* (Sakmann, B. and Neher, E., Eds.), pp 589–633, Plenum Press, New York.
- [17] Imoto, K., Busch, C., Sakmann, B., Mishina, M., Konno, T., Nakai, J., Bujo, H., Mori, Y., Fukuda, K. and Numa, S. (1988) *Nature* 335, 645–648.
- [18] Luetje, C.W. and Patrick, J. (1991) *J. Neurosci.* 11, 837–845.
- [19] Papke, R.L., Duvoisin, R.M. and Heinemann, S.F. (1993) *Proc. R. Soc. Lond. B Biol. Sci.* 252, 141–148.
- [20] Figl, A., Cohen, B.N., Quick, M.W., Davidson, N. and Lester, H.A. (1992) *FEBS Lett.* 308, 245–248.
- [21] Hussy, N., Ballivet, M. and Bertrand, D. (1994) *J. Neurophysiol.* 72, 1317–1326.
- [22] Cachelin, A.B. and Rust, G. (1995) *Pflügers Arch.* 429, 449–451.
- [23] Unwin, N. (1995) *Nature* 373, 37–43.
- [24] Gready, J.E., Ranganathan, S., Schofield, P.R., Matsuo, Y. and Nishikawa, K. (1997) *Protein Sci.* 6, 983–998.
- [25] Rajendra, S., Lynch, J.W., Pierce, K.D., French, C.R., Barry, P.H. and Schofield, P.R. (1995) *Neuron* 14, 169–175.